Second virial coefficients for dimethyl ether

Second Virial Coefficients for

Dimethyl Ether (DME)

Alessia Arteconi, Giovanni Di Nicola, Giulio Santori, Roman Stryjek

Dipartimento di Energetica, Università Politecnica delle Marche,

Via Brecce Bianche, 60100 Ancona, Italy

Abstract

Dimethyl Ether (DME) is a clean and economical alternative fuel. In addition it is also an ozone-friendly refrigerant. Burnett measurements were carried out at temperatures from (344 to 393) K and at pressures from (0.055 to 4.015) MPa. A total of 138 experimental points, taken along 15 isotherms and 12 different temperatures, were obtained. The apparatus was calibrated by helium. The derived second coefficients were compared with the selected correlations and with literature data.

tel:+39-0712204277

fax:+39-0712204770

Email: g.dinicola@univpm.it

Introduction

Dimethyl ether (DME) is the simplest ether, with a chemical formula of CH_3OCH_3. It is an important chemical material and it has many engineering applications. It is generally produced in a two step process: synthesis gas (syngas) is first converted to methanol and then DME is obtained by dehydration of methanol. The direct synthesis process technique from synthetic gas is still under development.[1] It can be made from coal, natural gas, residual oil, oil coke, and biomass and its production cost is rather low. In addition DME is non-toxic and non-carcinogenic.

Its physical properties are similar to those of liquefied petroleum gases (i.e., propane and butane), while burning DME, there are no emissions of SO_x, NO_x, or particulates. Its GWP is 0.3 per 100 years.[2]

Besides its use as an assistant solvent and an aerosol propellant, recently it was shown to be a good alternative fuel.[1] In addition, because of its favorable thermodynamic properties, it has been suggested as an alternative refrigerant (RE170). In particular for air conditioning applications, a mixture of mass fraction of 60 % ammonia and 40 % dimethyl ether forms an interesting azeotrope (R723).

For all these reasons, its thermophysical properties were recently studied[3] and a preliminary fundamental equation of state was derived.[4]

DME vapor pressure measurements were carried out at temperatures from (219 to 361) K and at pressures from (0.022 to 2.622) MPa, and a total of 71 experimental points were obtained in previous research at our laboratory.[5]

After a literature search, a very limited number of second virial coefficients for DME were found in the open literature.[6-11] In addition, the data are rather old and, excluding 2 points,[10] they were derived at a reduced temperature range that spans from 0.68 to 0.82. In this work, 138 experimental points were collected in the superheated vapor region and at higher reduced temperature range, spanning from 0.86 to 0.98. Derived second virial coefficients were compared with the predicted values by the Tsonopoulos correlating method.[12]

Experimental apparatus and procedures

The sample was provided by Aldrich Inc., USA. It was degassed by immersion in liquid nitrogen and evacuation. Its purity was checked by gas chromatography using a thermal conductivity detector and its mass fraction was found to be better than 99.8 % by analysis of peak area.

A diagram of the apparatus, since it is the same as described elsewhere,[13] is not reported here. It consisted of two pressure vessels, a measurement chamber, V_A, and an expansion chamber, V_B, with volumes of approximately (70 and 35) cm^3, respectively, and several auxiliary systems for filling and mixing the compounds in the Burnett vessels and for controlling and measuring the pressure and temperature. The measurement vessel was connected to a diaphragm-type differential pressure transducer (Ruska Model 2413) coupled to an electronic null indicator (Ruska Model 2416).

The pressure was regulated by a precision pressure controller (Ruska Model 3981), while a digital pressure indicator (Ruska Model 7000) was used to measure the pressure. Nitrogen is used as the pressure-transmitting fluid, and the nitrogen system consists of a reservoir, expansion vessels, and pressure regulating systems.

The vessels were immersed in a thermostatic bath filled with about 45 liters of silicon oil. The temperature of the bath was kept constant by means of a system with a PID device, controlled by a computer to which the temperature measurement system is also connected. The control and acquisition system relies on two platinum resistance thermometers calibrated according to ITS 90 at the Istituto Metrologico G. Colonnetti (IMGC) of Turin. In particular, for data acquisition and control measurements, a Hart Scientific Pt 25 resistance thermometer (Hart 5680) and a Tersid Pt 100 resistance thermometer were used, both connected to a digital temperature indicator (Corradi, RP 7000).

The Burnett constant, *N*, defined as the ratio of the volumes of cell A and the sum of the volumes of cells A and B at zero pressure, was found to be $N = 1.5220 \pm 0.0001$ for present measurements.

Measurements were performed using the classical Burnett experimental procedure. Initially, the first vessel was filled with the sample and its temperature and pressure were measured. Then, after evacuating the second vessel, the expansion valve was opened. Once the pressures between the vessels had equalized, the second vessel was isolated and evacuated again. This procedure was repeated until low pressures were achieved.

The uncertainty in the temperature measurements is due to the thermometer and any instability of the bath. The stability of the bath was found to be better than ±0.015 K, and the uncertainty of the thermometer was found to be better than 0.010 K in our temperature range. The total uncertainty in the temperature measurements was thus less than 0.025 K.

The uncertainty in the pressure measurements is due to the transducer and null indicator system, and to the pressure gages. The digital pressure indicator (Ruska Model 7000) has an uncertainty of ±0.003 % of full scale. The total uncertainty in the pressure measurement is also influenced by temperature fluctuations due to bath instability and was found to be less than ±1 kPa.

Results

The second and third virial coefficients obtained from the Burnett expansions of helium are reported in Table 1 together with deviations obtained from the McCarty equation of state.[14] Results showed a good agreement with reference data[14] in terms of the second virial coefficients (AAD=0.9 cm^3/mol) and slightly poorer in terms of the third virial coefficients (AAD=321 cm^6/mol^2). However, in terms of pressure an AAD=0.125 kPa was obtained.

For DME, in total 138 experimental points were collected along 15 isotherms in a temperature range from (344 to 393) K and for pressures from (0.055 to 4.015) MPa. Adopting the critical temperature value of T_c = 400.3 K,[16] the experimental reduced temperature range spanned from 0.86 to 0.98. The experimental data are shown in Table 2.

The experimental *PVT* measurements were used to derive the second, *B*, and third, *C*, virial coefficients of the virial equation,

$$P = \frac{RT}{V}\left(1 + \frac{B}{V} + \frac{C}{V^2}\right) \quad (1)$$

In the regression, each run was treated separately and $(dP)^2$ was used as an objective function applying the Burnett constant from the helium calibration.

Defining the average absolute deviation in pressure as

$$\mathrm{AAD} = \sum_{i=1}^{N} \mathrm{abs}(dP) / N \quad (2)$$

we found *AAD* = 0.63 kPa, well within the estimated experimental uncertainty. The second and third virial coefficients are shown in Table 3, together with the pressure deviations from the fit.

The second virial coefficients (*B*) are also reported in Figure 1. This figure shows that the second virial coefficients, especially for values at $T_r < 0.92$, are rather scattered. This was probably caused from the small pressure range, limited by the saturation pressure of DME. This limitation also produced scattered values at low reduced temperatures for the third virial coefficients.

In order to overcome this problem, data were refitted keeping the third virial coefficients as fixed values according to the Orbey and Vera correlating method.[16] The resulting values for the second virial coefficients, *B'*, and initial density, ρ (1), are also reported in Table 3.

The *B'* were plotted in Figure 1 together with second virial coefficients calculated by eq 1 as described above (*B*). Even if from the analysis of the deviations for reproducing the pressures by the different methods the *B'* values appear to have a slightly higher AAD, comparing the *B'* with the *B* values, a significant improvement was evident, especially at lower reduced temperatures, where the obtained *B'* values were clearly less scattered than the *B* values. For this reason the *B'* were taken as reference values and fitted according to the following temperature function:

$$B' = b_o + b_1/T_r \quad (3)$$

with b_o = 350.3812 $cm^3 \cdot mol^{-1}$ and b_1 = -565.7195 $cm^3 \cdot K \cdot mol^{-1}$. Eq 3 predicts the *B'* values with and AAD = 3.2 $cm^3 \cdot mol^{-1}$. The second virial coefficients calculated by eq 3 are also reported in Figure 1 as a dashed line.

In Figure 2, the second virial coefficients (*B'*) are plotted over a different reduced temperature scale and compared with values reported in the literature.[6] In the Figure, the values predicted by the Tsonopoulos[7] correlating method are also shown. Considering that the literature second virial coefficients were generally obtained at very different temperatures and that only two points were obtained (by one of us) about four decades ago at our reduced temperature range (from 0.86 to 0.98), the trend of the present results can be considered satisfactory.

The uncertainties in the second virial coefficients, estimated on statistical base, are of about 4 $cm^3 \cdot mol^{-1}$.

If the data from the Burnett expansions cover only low pressures and the number of expansions are limited, it may not be possible to tune all three parameters, namely *B*, *C* and ρ (1), especially considering the real accuracy in the pressures measurements. Moreover, the contribution from the third virial coefficient to the values of the compressibility is much smaller than from the second virial coefficient, hence it may be better to use an alternative method for the Burnett data reduction. Keeping in mind that the contribution from the third virial coefficient is very small but not negligible, we choose the option of "a priori" estimation from one of the predictive methods of the values of the third virial coefficients, thus tuning only two parameters, namely *B* and ρ (1). After testing, we choose the third virial coefficients from the Orbey and Vera method: in this way *B'* and ρ' (1) are considered as the most acceptable from our experimental data.

The eventual adsorption contribution should be detected while plotting P_i/P_{i+1}. The Burnett ratio P_i/P_{i+1} was reported in Figure 3 for three runs obtained at different temperatures and taken as example. The adsorption should be greater at lower temperatures, what is not evident from the graph.

Conclusions

The *PVT* properties of an important alternative fuel such as DME were measured at temperatures from (344 to 393) K. The second and third virial coefficients were derived and compared with

empirical correlating methods and with data found in the literature. After different attempts, we decided to fix the third virial coefficients according to the Orbey and Vera correlating method. The second virial coefficients derived in this way followed approximately the same trend as the literature ones that were obtained at a different reduced temperature range.

References

1. Semelsberger, T. A.; Borup, R. L.; Greene, H. L. Dimethyl ether (DME) as an alternative fuel. *J. Pow. Sour*. **2006**, *156*, 497–511.

2. Good, D. A.; Francisco, J. S.; Jain, A. K.; Wuebbles, D. J. Lifetimes and global warming potentials for Dimethyl Ethers and for Fluorinated Ethers: CH_3OCF_3 (E143a), CHF_2OCHF_2 (E134), CHF_2OCF_3 (E125). *J. Geophys. Res.* **1998**, *103*, 28181–28186.

3. Liu, Z.; Wu, J. Researches on the Thermophysical Properties of Alternative Fuel, Proceedings of the 8th Asian Thermophysical Properties Conference, 21 - 24 August, **2007**, Fukuoka, Japan.

4. Ihmels, E. C.; Lemmon, E. W. Experimental densities, vapor pressures, and critical point, and a fundamental equation of state for dimethyl ether. *Fluid Phase Equilib*. **2007**, *260*, 36-48.

5. Corvaro, F.; Di Nicola, G.; Polonara, F.; Santori, G. Saturated Pressure Measurements of Dimethyl Ether at Temperatures from (219 to 361) K. *J. Chem. Eng. Data* **2006**, *51*, 1469-1472.

6. Dymond, J. H.; Marsh, J. H.; Wilhoit, R. C.; Wong, K. C. Virial Coefficients of Pure Gases, Part A. Landolt-Börnstein, New Series IV/21A, **2002**.

7. Cawood, W; Petterson, H. S. The compressibilites of certain gases at low pressures and various temperatures. *J. Chem. Soc.* **1933**, *156*, 619-624.

8. Kennedy, R. M.; Sagen-Kahn, M.; Aston, J. G. The heat capacity and entropy, heats of fusion and vaporisation, and the vapour pressure of dimethyl ether. *J. Am. Chem. Soc.* **1941**, *63*, 2267-2272.

9. Tripp, T. B.; Dunlap, R. D. Second virial coefficients for the systems: n-butane+perfluoro-n-butane and dimethyl ether+1,hydroperfluorpropane. *J. Phys. Chem.* **1962**, *66*, 635-639.

10. Osipiuk, B.; Stryjek, R. Second virial coefficients of binary methyl *n*-Alkyl ether-sulphur dioxide mixtures. *Bull. Acad. Polon. Sci. Ser. Sci. Chim*. **1970**, *18*, 289-295.

11. Haworth, W. S.; Sutton, L. E. Equilibrium properties of polar gases. Part 1. The second density virial coefficients of some polar gases. *Trans. Faraday Soc.* **1971**, *67*, 2907-2914.

12. Tsonopoulos, C. An empirical correlation of second virial coefficients, *AIChE J.* **1974**, *20*, 263-272.

13. Di Nicola, G.; Polonara, F.; and Stryjek. R. Burnett Measurements for the Difluoromethane + Carbon Dioxide System. *J. Chem. Eng. Data* **2002**, *47*, 876-881.

14. McCarthy, R. D. Thermodynamic Properties of Helium 4 from 2 to 1500 K at Pressures to 10^8 Pa. *J. Phys. Chem. Ref. Data* **1973**, *2*, 923-1042.

15. Lemmon, E. W.; Huber, M. L.; McLinden, M. O. NIST Standard Reference Database 23, Reference Fluid Thermodynamic and Transport Properties (REFPROP), version 8.0 (National Institute of Standards and Technology), **2007**.

16. Orbey, H; Vera, J. H. Correlation for the third virial coefficient using T_c, P_c and ω as parameters. *AIChE J.* **1983**, *29*, 107-113.

Table 1. Second (B) and third (C) virial coefficients for helium; $\rho(1)$ denote regressed initial densities.

Series	T /K	B /cm^3·mol^{-1}	abs (dB) /cm^3·mol^{-1}	C /cm^6·mol^{-2}	abs (dC) /cm^6·mol^{-2}	ρ (1) /mol·dm^{-3}	abs (dP) /kPa	bias (dP) /%
1	343.87	10.6	1.2	534	535	1.98072	0.239	0.051
2	343.87	9.7	2.1	905	906	1.80089	0.271	0.066
3	354.02	11.0	0.7	427	428	1.87893	0.156	0.039
4	354.12	11.5	0.2	272	273	1.87300	0.138	0.034
5	363.36	12.8	1.1	-146	145	1.90409	0.072	-0.009
6	364.36	11.9	0.2	135	136	1.88208	0.051	0.013
7	374.64	12.4	0.8	-10	9	1.85374	0.035	0.008
8	374.65	12.8	1.2	-140	139	1.85231	0.040	-0.002
AAD			0.9		321		0.125	0.033

Table 2. Experimental pressures measured during Burnett expansions of DME.

Series 1		Series 2		Series 3		Series 4		Series 5	
T/K		*T*/K		*T*/K		*T*/K		*T*/K	
343.86		343.86		343.86		348.96		354.08	
P/MPa	ρ/mol·dm^{-3}	*P*/MPa	ρ/mol·dm^{-3}	*P*/MPa	ρ/mol·dm^{-3}	*P*/MPa	ρ/mol·dm^{-3}	*P*/MPa	ρ/mol·dm^{-3}
1.3265	0.5535	1.3654	0.5744	1.6973	0.7651	1.5747	0.6794	1.7013	0.7260
0.9286	0.3637	0.9589	0.3774	1.2256	0.5027	1.1211	0.4464	1.2129	0.4770
0.6340	0.2390	0.6564	0.2480	0.8510	0.3303	0.7749	0.2933	0.8392	0.3134
0.4280	0.1570	0.4427	0.1629	0.5784	0.2170	0.5261	0.1927	0.5699	0.2059
0.2857	0.1032	0.2958	0.1070	0.3890	0.1426	0.3534	0.1266	0.3827	0.1353
0.1898	0.0678	0.1966	0.0703	0.2592	0.0937	0.2358	0.0832	0.2552	0.0889
0.1257	0.0445	0.1302	0.0462	0.1718	0.0616	0.1567	0.0547	0.1694	0.0584
0.0831	0.0293	0.0861	0.0304	0.1137	0.0404	0.1039	0.0359	0.1122	0.0384
0.0550	0.0192	0.0570	0.0199	0.0751	0.0266	0.0689	0.0236	0.0743	0.0252

Series 6		Series 7		Series 8		Series 9		Series 10	
T/K		*T*/K		*T*/K		*T*/K		*T*/K	
359.21		364.35		364.36		369.49		374.64	
P/MPa	ρ/mol·dm^{-3}	*P*/MPa	ρ/mol·dm^{-3}	*P*/MPa	ρ/mol·dm^{-3}	*P*/MPa	ρ/mol·dm^{-3}	*P*/MPa	ρ/mol·dm^{-3}
2.0459	0.9065	2.2596	0.9953	2.4857	1.1491	1.9759	0.8077	2.7299	1.2338
1.4868	0.5956	1.6477	0.6540	1.8485	0.7550	1.4070	0.5307	2.0291	0.8107
1.0408	0.3913	1.1557	0.4297	1.3092	0.4960	0.9736	0.3487	1.4405	0.5326
0.7124	0.2571	0.7903	0.2823	0.9019	0.3259	0.6616	0.2291	0.9948	0.3500
0.4809	0.1689	0.5345	0.1855	0.6107	0.2141	0.4446	0.1505	0.6751	0.2299
0.3218	0.1110	0.3572	0.1219	0.4090	0.1407	0.2966	0.0989	0.4532	0.1511
0.2142	0.0729	0.2373	0.0801	0.2721	0.0924	0.1970	0.0650	0.3021	0.0993
0.1420	0.0479	0.1571	0.0526	0.1802	0.0607	0.1305	0.0427	0.2004	0.0652
0.0941	0.0315	0.1038	0.0346	0.1191	0.0399	0.0862	0.0281	0.1326	0.0428

Series 11		Series 12		Series 13		Series 14		Series 15	
T/K		*T*/K		*T*/K		*T*/K		*T*/K	
379.80		384.95		390.14		390.15		393.24	
P/MPa	ρ/mol·dm^{-3}	*P*/MPa	ρ/mol·dm^{-3}	*P*/MPa	ρ/mol·dm^{-3}	*P*/MPa	ρ/mol·dm^{-3}	*P*/MPa	ρ/mol·dm^{-3}
3.1183	1.4494	3.5918	1.7846	3.7219	1.7780	3.9365	2.0082	4.0152	1.9932
2.3529	0.9523	2.7910	1.1725	2.8615	1.1682	3.0949	1.3195	3.1377	1.3096
1.6872	0.6257	2.0457	0.7704	2.0770	0.7676	2.2913	0.8670	2.3023	0.8605
1.1718	0.4111	1.4294	0.5062	1.4540	0.5043	1.6144	0.5696	1.6238	0.5654
0.7979	0.2701	0.9803	0.3326	0.9952	0.3314	1.1134	0.3743	1.1169	0.3715
0.5365	0.1775	0.6622	0.2185	0.6714	0.2177	0.7554	0.2459	0.7561	0.2441
0.3579	0.1166	0.4431	0.1436	0.4489	0.1430	0.5070	0.1616	0.5067	0.1604
0.2375	0.0766	0.2946	0.0943	0.2984	0.0940	0.3380	0.1062	0.3373	0.1054
0.1571	0.0503	0.1951	0.0620	0.1975	0.0617	0.2244	0.0697	0.2235	0.0692
0.1038	0.0331	0.1289	0.0407					0.1477	0.0455

Table 3. Second (B and B') and third (C) virial coefficients for DME; $\rho(1)$ and $\rho'(1)$ denote regressed initial densities.

	T /K	B /cm^3·mol^{-1}	C /cm^6·mol^{-2}	ρ (1) /mol·dm^{-3}	abs (dP) /kPa	bias (dP) /%	B' /cm^3·mol^{-1}	ρ' (1) /mol·dm^{-3}	abs (dP') /kPa	bias (dP') /%
Series										
1	343.86	-301	15190	0.55367	0.232	0.128	-302	0.55355	0.234	0.100
2	343.86	-293	1770	0.57356	0.158	0.124	-303	0.57440	0.266	0.032
3	343.86	-274	-17560	0.75968	0.270	0.089	-306	0.76514	1.016	-0.224
4	348.96	-323	34880	0.68182	0.390	0.217	-308	0.67942	0.521	0.316
5	354.08	-301	24820	0.72744	0.239	0.139	-294	0.72604	0.264	0.176
6	359.21	-296	26570	0.90953	0.392	0.153	-286	0.90653	0.589	0.244
7	364.35	-267	15860	0.99792	0.284	0.042	-269	0.99531	0.287	0.000
8	364.36	-257	8430	1.14436	0.062	0.000	-269	1.14906	1.047	-0.194
9	369.49	-280	30970	0.81090	0.291	0.122	-266	0.80774	0.589	0.235
10	374.64	-260	20150	1.24000	0.300	0.077	-256	1.23379	0.496	0.131
11	379.80	-246	18010	1.45152	0.106	0.012	-244	1.44945	0.200	0.031
12	384.95	-236	15670	1.78343	1.576	-0.037	-237	1.78459	1.736	-0.110
13	390.14	-229	16790	1.77933	0.086	0.002	-229	1.77798	0.105	-0.005
14	390.15	-238	19720	2.02045	1.777	0.035	-230	2.00824	2.868	0.233
15	393.24	-228	17740	1.99930	0.207	0.047	-225	1.99319	0.976	0.137
AAD					0.420	0.080			0.750	0.140

.

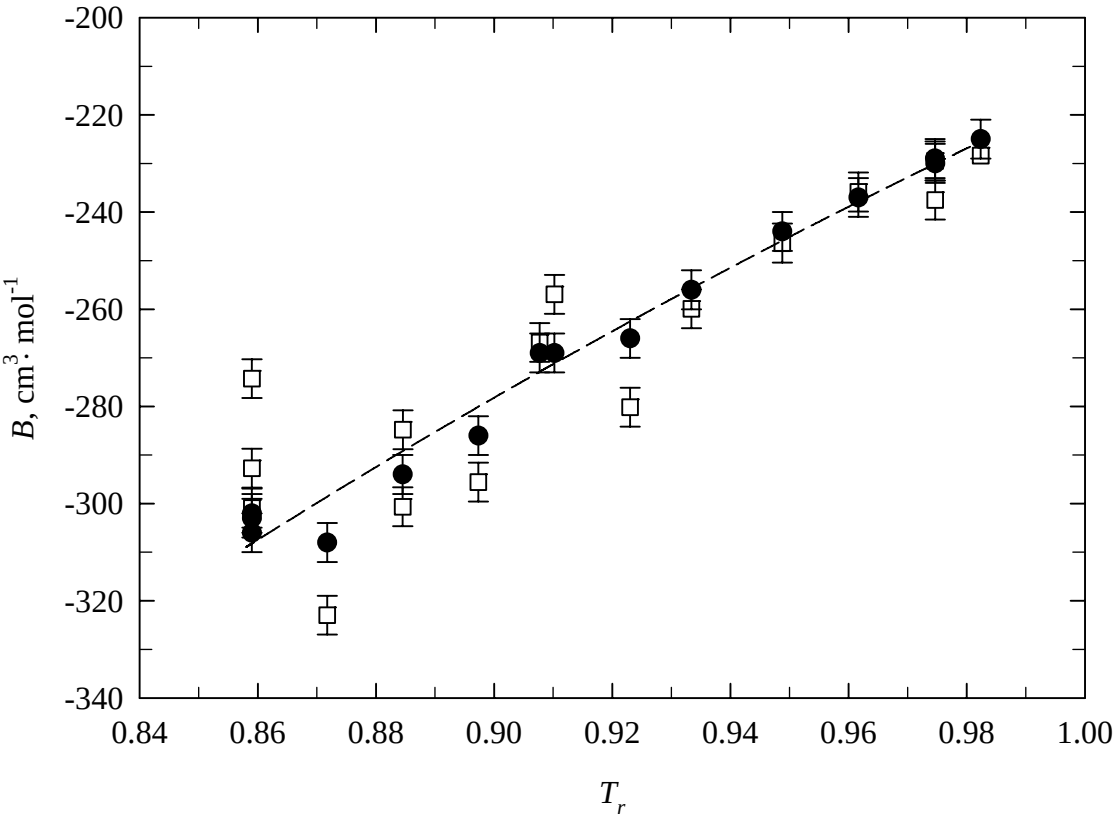

Figure 1. Second virial coefficients, B = (□) and B' = (●), against reduced temperature. The values fitted by equation (3) are presented by a dashed line.

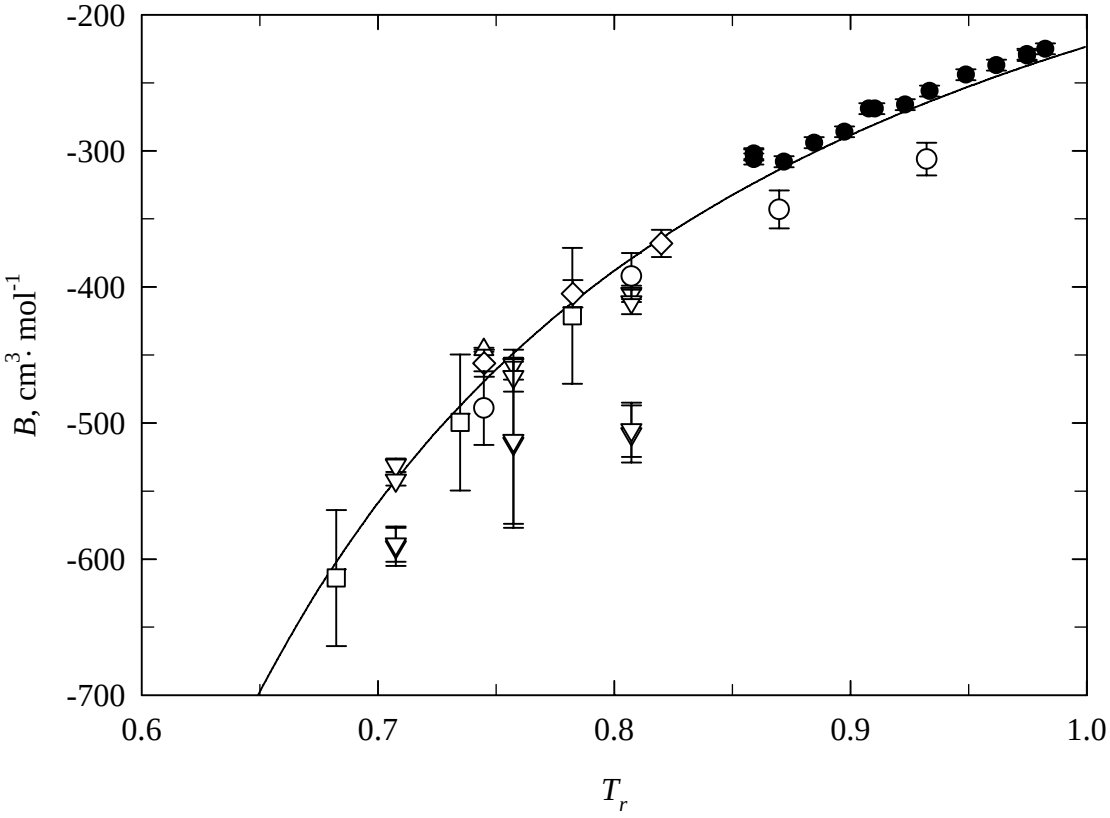

Figure 2. Second virial coefficients, *B'*, against reduced temperature. The values correlated by the Tsonopoulos[7] correlating method are presented by a solid line.

●, Present work; □, ref 7; △, ref 8; ▽, ref 9; ○, ref 10; ◇, ref 11.

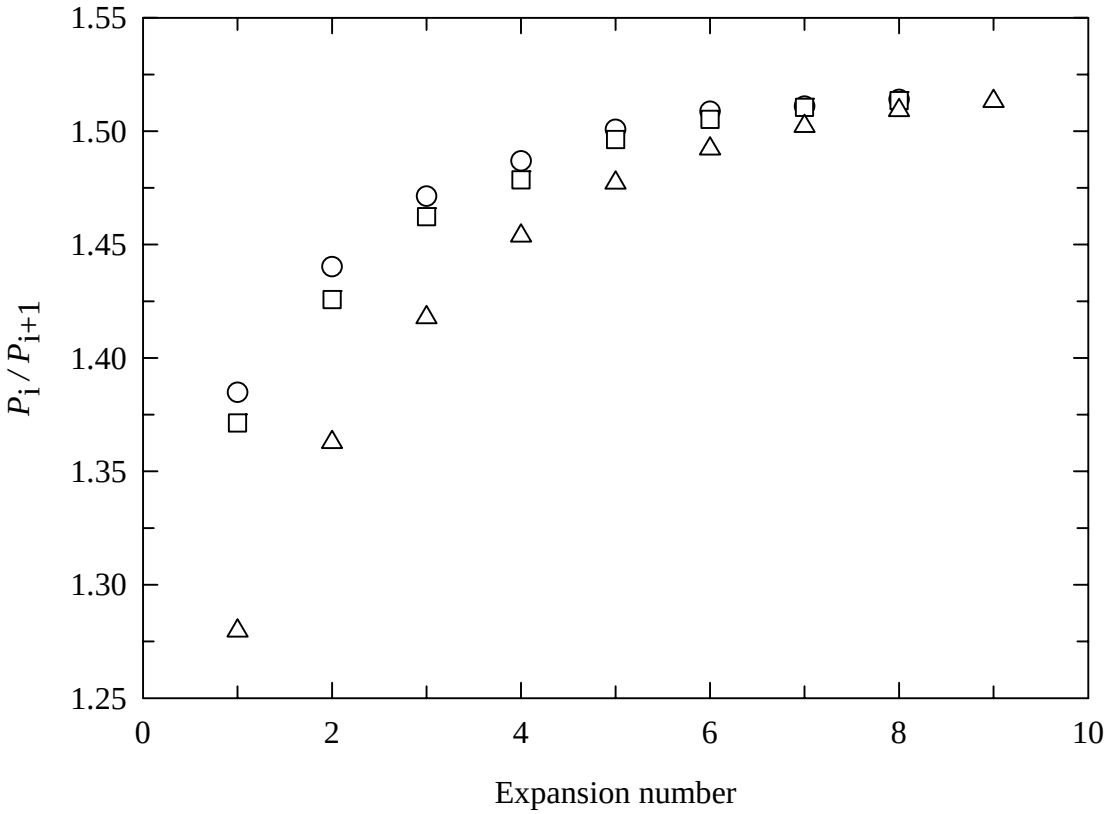

Figure 3. P_i/P_{i+1} against the expansion number for three runs.

○, T = 343.86 (series 3); □, T = 364.35 K (series 7); △, T = 393.24 K (series 15).